Modification of atom scattering using an intercombination-line optical Feshbach resonance at large detuning

Y. N. Martinez de Escobar†, P. G. Mickelson†, M. Yan, and T. C. Killian
Rice University, Department of Physics and Astronomy and Rice Quantum Institute, Houston, Texas, 77251
(Dated: June 9, 2009)

We demonstrate control of the scattering properties of atomic strontium with an optical Feshbach resonance near the $^1S_0$-$^3P_1$ intercombination transition at 689 nm. Significant changes in scattering length on the order of $\pm 10\, a_0$ can be achieved at large detuning ($\sim 10^6$ linewidths), and we are able to increase phase space density through enhanced evaporative cooling. Loss rate constants are at least two orders of magnitude smaller than in previous experiments with optical Feshbach resonances, but are three orders of magnitude larger than predicted.

The ability to tune interactions in quantum atomic gases makes these systems ideal for exploring many-body physics [1] and has enabled some of the most important recent advances in atomic physics, such as investigation of the BEC-BCS crossover regime [1] and creation of quantum degenerate molecules [2, 3]. Magnetic Feshbach resonances [4], which are the standard tool for changing atomic interactions, have proven incredibly powerful, but they are also limited because the methods for creating magnetic fields preclude high-frequency spatial and temporal modulation.

Here, we demonstrate tuning atom interactions with an optical Feshbach resonance (OFR) [5] in ultracold atomic strontium. Using light, it should be possible to manipulate interactions on time scales as short as a femtosecond and spatial scales as fine as an optical wavelength. By exploiting the regime of large detuning from a narrow intercombination optical transition, we demonstrate much lower atom loss rates than seen in previous OFR experiments [6, 7, 8, 9], which will open new avenues of research in non-linear physics, quantum optics, and condensed matter physics, such as stabilization of matter-wave solitons in two dimensions [10], controlled emission from a matter-wave laser [11], and creation of quantum fluids with random non-linear interactions [12].

In a Feshbach resonance, the scattering state of colliding atoms couples to a bound molecular state, resulting in significant enhancements of elastic and inelastic collision cross sections when the free and bound states are in resonance. In an OFR, coupling is created by a laser driving a photoassociative resonance between colliding atoms and an excited molecular level. Previous observations of OFRs [6, 7, 8] used strong dipole-allowed transitions in alkali-metal atoms to alter atomic collision properties, but substantial change in the atom-atom scattering length was accompanied by rapid atom loss. For example, Theis *et al.* [7] found that for a scattering length change of $\pm 90\ a_0$ ($a_0 = 5.29 \times 10^{-11}\,\mathrm{m}$), large inelastic-loss rate constants ($\beta_{in} \approx 10^{-10}\ \mathrm{cm}^3/\mathrm{s}$) limited observation times to less than $100\,\mu\mathrm{s}$, which is insufficient for applications [10, 11, 12]. Similar results, but with about two orders of magnitude lower loss, were obtained for a magnetic Feshbach resonance using an AC Stark shift of the closed channel to modify the position of the resonance [13].

Ciurylo *et al.* [14, 15] predicted that an OFR induced by a laser tuned near a weakly allowed transition should tune the scattering length with significantly less induced loss. This can be done with alkaline-earth atoms, or atoms with similar atomic structure such as Ytterbium (Yb), by exciting near an intercombination transition from the singlet ground state to a metastable triplet level. The improved OFR properties result from the long lifetime of the excited molecular state and relatively large overlap integral between excited molecular and ground collisional wave functions.

An OFR driven with an intercombination transition was recently investigated in Yb [9]. Very large changes in the scattering length were inferred from changes in the photoassociative loss spectrum. However, observed loss rate constants were still on the order of $10^{-11}\ \mathrm{cm}^3/\mathrm{s}$ because the OFR laser detuning was kept small ($\Delta \simeq 100$ MHz), similar to alkali atom experiments [6, 7, 8]. This experiment did not test the scaling of loss and scattering-length-change with detuning, nor did it examine the large detuning limit in which losses are expected to be small; both are crucial for applications.

We investigate the large detuning regime of an optical Feshbach resonance driven with an intercombination transition in ^{88}Sr and directly probe the effect on the elastic collision rate. The OFR laser is tuned near the $^1S_0$-$^3P_1$ transition at 689 nm. Significant changes in scattering length on the order of $\pm 10\, a_0$ can be achieved, in agreement with theory [14, 15], and loss rate constants are at least two orders of magnitude smaller than in previous experiments [9, 14, 15]. Large detuning from molecular resonance is defined by the condition [14]

$$|\Delta| \gg \Gamma_{mol} + \Gamma_{stim}. \tag{1}$$

Here, Δ is the detuning of the OFR laser, of intensity I, from an excited molecular level that has a natural linewidth $\Gamma_{mol} = 1 \times 10^5\,\mathrm{s}^{-1}$. $\Gamma_{stim} \propto I$ is the laser-stimulated linewidth resulting from the coupling of the excited level to the ground state of colliding atoms.

The OFR laser modifies the atomic scattering length according to $a(\Delta, I) = a_{bg} + a_{opt}(\Delta, I)$, where a_{bg} is the background scattering length in the absence of laser light,

and

$$a_{opt}(\Delta, I) = l_{opt}\frac{\Gamma_{mol}}{\Delta} \tag{2}$$

is the optically induced part of the scattering length for large detuning. The "optical length" l_{opt}, a parameter characterizing the strength of the OFR, is proportional to I and defined as

$$l_{opt} = \frac{\Gamma_{stim}}{2k_r\Gamma_{mol}}, \tag{3}$$

where $k_r = \sqrt{2\mu\varepsilon_r}/\hbar$, $\mu = m/2$ is the reduced mass, ε_r is the kinetic energy of the colliding atom pair, and $\hbar$ is Planck's constant divided by 2π. The elastic collision cross section determines the cooling power of evaporation in ultracold gases, and it varies with the square of a,

$$\sigma = 8\pi(a_{opt} + a_{bg})^2. \tag{4}$$

The Feshbach laser also induces two-body inelastic collisional losses, which are described by the loss rate constant $\beta_{in}(\Delta, I)$,

$$\beta_{in}(\Delta, I) = \frac{4\pi\hbar}{\mu}l_{opt}\left(\frac{\Gamma_{mol}}{\Delta}\right)^2. \tag{5}$$

$\beta_{in}(\Delta, I)$ is defined such that it contributes to density evolution as $\dot{n} = -\beta_{in}(\Delta, I)n^2$.

The ground and excited molecular potentials in Sr are well-characterized from FTIR spectroscopy [16] and one- [17, 18, 19] and two-photon [20] photoassociation experiments. In ^{88}Sr, the least-bound state of the molecular $^1S_0$+$^3P_1$ potential is bound by only 400 kHz with respect to the asymptotic energy of a free $^1S_0$ and $^3P_1$ atom pair, which leads to an extremely large l_{opt} for $I = 1\,\mathrm{mW/cm^2}$ of $4.5 \times 10^2\,a_0$ [19]. l_{opt} decreases rapidly with increasing binding energy of the molecular state, and coupling to the least-bound level dominates the OFR effect even at large red detunings ($\Delta/2\pi \geq 1\,\mathrm{GHz}$) for which there are other molecular levels at smaller detuning. Equations (2) and (5) predict that for laser intensities on the order of 15 W/cm^2 ($\Gamma_{stim}/2\pi \approx 10^8\,\mathrm{Hz}$) and detunings of $\pm 10\,\mathrm{GHz}$, the ^{88}Sr scattering length can be changed by $a_{opt} = \pm 10\,a_0$ with a loss rate constant of only $\beta_{in} = 10^{-17}\,\mathrm{cm^3/s}$. This change in scattering length is reasonable in absolute terms, but is also very large in relative terms because for ^{88}Sr, a_{bg} is very close to zero [20]. The fortunate occurrence of a large l_{opt} and small a_{bg} makes ^{88}Sr ideal for exploiting an OFR.

To determine the effect of the OFR on elastic and inelastic collision properties, we measured the evolution of the number of atoms and temperature for samples held in a crossed optical dipole trap (ODT) using time-of-flight absorption imaging as previously described in [20]. The OFR laser is applied after an equilibration time of 60 ms in the ODT, and it remains on during a variable hold time ($0.1 - 5\,\mathrm{s}$) until the ODT beams are extinguished and the atoms are released, at which time the OFR laser is also blocked. Initial conditions in the ODT, which depend on the trap depth, are approximately $4 - 15 \times 10^6$ atoms and $3 - 10\ \mu$K. Trap frequencies for the ODT were measured using a parametric oscillation drive technique [21] and range between 100 and 500 Hz.

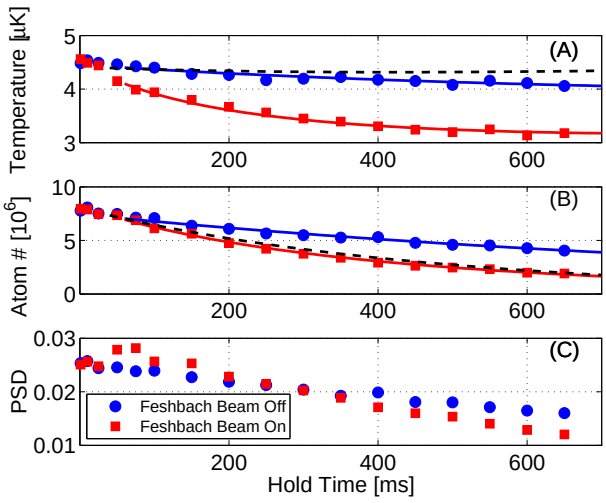

FIG. 1: Atom sample evolution and model fits with and without the OFR laser. The initial peak density is $4 \times 10^{13}\,\mathrm{cm^{-3}}$ and the trap depth is $7.5\,\mu$K. (A) The sample temperature drops in the presence of the OFR beam (I = 24 W/cm^2, $\Delta/2\pi = -2.5\,\mathrm{GHz}$), indicating an increase in elastic collision cross section and efficiency of evaporative cooling. (B) The number of atoms decreases more quickly due to losses induced by the OFR laser, but the sample lifetime is still approximately 500 milliseconds. (C) The peak phase space density (PSD) initially increases. Solid lines are fits using the model described in the text. The dashed line is the modeled evolution including heating and losses due to the OFR laser but assuming the elastic cross section does not increase.

We produce the OFR beam by injection-locking a slave diode with the output of a stable master ECDL in a Littman-Metcalf configuration (linewidth below 1 MHz). The detuning from the OFR molecular resonance is measured with an accuracy of 100 MHz with a Fabry-Perot reference cavity. The OFR laser was applied to the atoms in a single-pass running wave with a beam waist of 228 μm and a peak intensity of about 38 W/cm^2 for the maximum output power of 31 mW.

Figure 1A shows the use of an OFR at large detuning to tune the elastic collision and thermalization rates. Samples are held in a crossed optical dipole trap (ODT). The OFR laser increases the elastic collision cross section and enables more efficient evaporative cooling, causing the temperature to drop in comparison to when no OFR laser is present. Atom losses due to the OFR are also apparent, but the long time scale of atom loss of approximately 500 ms is a significant improvement over previous experiments with OFRs [6, 7, 8], allowing a slight increase in phase space density.

To quantify the effect of the OFR, we numerically

model the evolution of atom number and total sample energy following the formalism of Comparat *et al.* [22], which adapts the evaporative cooling treatment of [23] to describe evaporation, two-body inelastic losses due to the OFR laser, heating due to photon scattering from the ODT and OFR lasers, and one-body losses due to background gas collisions and scattering of OFR laser photons. The main assumptions are ergodicity and a truncated Boltzmann distribution for the atom velocity distribution. Because the ^{88}Sr elastic cross section is small, the ratio of trap depth to temperature is relatively small, $\eta \approx 2-4$. Combined with the lack of spatial symmetry in the ODT, this precludes the use of normal approximations that simplify expressions for heating, cooling, and loss processes [22, 24, 25]. Reference [26] describes the full numerical calculation developed to handle this situation, which allows extraction of elastic and inelastic collisional rate constants from data such as that shown in Fig. 1.

With no OFR laser we derive an elastic collision cross section of $\sigma = 600\, a_0^2$. Data with longer hold times allow clear separation of one- and two-body loss contributions and show that β_{in} is negligible if the OFR laser is absent, and that it can be set equal to zero. This yields a one-body loss rate of approximately $1\, s^{-1}$, consistent with background collisions.

The small negative value of $a_{bg} = -1.4(6)\, a_0$ for ^{88}Sr in the limit of vanishing collision energy leads to significant variation of the cross section with energy (Fig. 2A) [20]. This complicates comparison of theory and experiment because a distribution of collision energies contributes in the thermal sample in the ODT; a full energy-dependent calculation is beyond the scope of this study. We treat this phenomenon in approximate fashion by forming an effective, temperature-dependent cross section, $\langle\sigma\rangle$, that is an average of the collision-energy dependent cross section $\sigma\,(E_{coll})$, where the weighting is the relative contribution of collisions of each energy to the total collision rate per volume in the sample (Z) [26]. This yields $\langle\sigma\rangle = Z/(2n_0^2\sqrt{\frac{k_B T}{\pi m}})$, where k_B is Boltzmann's constant, n_0 is atom density, and T is the temperature. Here, Z is calculated using the theoretical energy dependence of σ [20] and, for simplicity, an untruncated velocity distribution [27]

$$Z = \frac{2\pi n_0^2}{\mu}\int dp\, p^3 \frac{\sigma\,(E_{coll})}{(2\pi\mu k_B T)^{3/2}} e^{-\frac{p^2}{2\mu k_B T}}, \qquad (6)$$

where the collision energy is $E_{coll} = \frac{p^2}{2\mu}$ for relative momentum p. We find agreement between observed and theoretical cross section values (Fig. 2A), giving confidence in the numerical model of collision dynamics.

Figure 2B shows that with the application of an OFR laser, the collision cross section varies quadratically with I/Δ, as expected from Eqs. (2) and (4). The largest value of $\langle\sigma\rangle$ observed is approximately $\langle\sigma\rangle = 5000\, a_0^2$. Even though the experiment does not access the low-

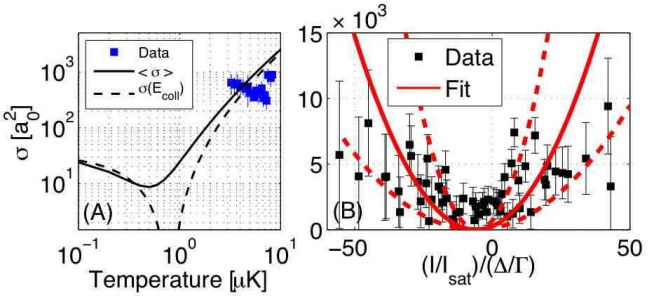

FIG. 2: (A) Variation of the ^{88}Sr collision cross section with collision energy or temperature in the absence of an OFR laser. The dashed curve gives the variation of cross section with collision energy [20], where collision energy is set to $2k_BT$, the average collision energy for temperature T. The solid curve is an average of the cross section over collision energies as a function of sample temperature as described in the text. (B) The elastic collision cross section versus the scaling parameter, I/Δ. Error bars reflect statistical variation. The solid line is a fit to Eq. (4), with confidence intervals marked by the dashed lines.

energy limit in which the scattering length is strictly defined, for clarity we will characterize the cross section with an effective scattering length according to Eq. (4). We thus infer a maximum of $|a| = 14\, a_0$, which is a significant change from a_{bg}. The fit yields an optical length for $I = 1\,\mathrm{mW/cm^2}$ of $l_0 = 1.7^{+1.3}_{-0.7} \times 10^2\, a_0$. Quoted uncertainties are statistical. In addition, there is a factor of two uncertainty arising from 20% uncertainty in the optical trap oscillation frequencies, so there is reasonable agreement with the value determined from the intensity of the photoassociation spectrum [9].

The curve in Fig. 2B is not centered on zero, which reflects the fact that $a_{bg} \neq 0$. The fit yields $a_{bg} = 3\, a_0$, in good agreement with the value expected for samples in this temperature range (Fig. 2A). Negative detuning is required to create an $a_{opt} < 0$ and a minimum in the cross section. We suspect that the discrepancy between data and theory near the minimum results from our simplified treatment of the energy dependence of the cross section.

The two-body inelastic loss rate constant β_{in} (Eq. (5)) is also determined from the model fit as shown in Fig. 1. At low values of the intensity, β_{in} is small, and there is too much correlation between the one- and two-body losses to determine β_{in} well. We overcome this problem by determining β_{in} for larger intensities and using a linear fit of β_{in} to determine the values at lower intensity (Fig. 3A), which are held constant while fitting other parameters in the collisional dynamics model.

The measured β_{in}/I values roughly follow a $1/\Delta^2$ dependence as predicted by Eq. (5) (Fig. 3B), with $\beta_{in}/I = 4 \times 10^{-14}/[\Delta/2\pi(\mathrm{GHz})]^2$ ($\mathrm{cm^5/Ws}$). Fluctuations in the data lead to a factor of two statistical uncertainty, in addition to the factor of two systematic uncertainty from determination of the optical trap oscillation frequencies. This value of β_{in}/I is approximately 1000

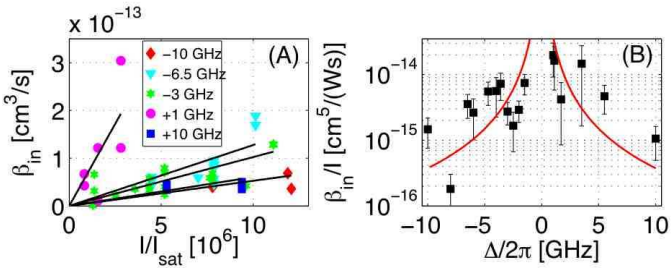

FIG. 3: (A) Variation of β_{in} with OFR laser intensity and detuning. One- and two-body losses are strongly correlated for low intensities so we determine β_{in} for large intensities and use these linear fits to extrapolate to lower values. (B) Frequency dependence of β_{in}/I. Error bars reflect statistical variation. The solid line is a fit to Eq. (5).

times larger than one would expect from the value of l_{opt} determined in Fig. 2A, and the cause of this discrepancy is an open question. At smaller detunings and larger loss rates, it was found that losses do follow theoretical predictions [7, 8, 9]. It was suggested [19] that off-resonant scattering on the atomic $^1S_0$-$^3P_1$ transition would be a concern for using the OFR at large detuning in Sr. Light-assisted collisional processes that stimulate this transition may also contribute to the larger-than-expected β_{in}. Alternatively, the two-level theory for an OFR [14, 15] may require modification in the regime of large detuning.

We have used a laser detuned far from molecular resonance near the weakly allowed $^1S_0$-$^3P_1$ intercombination line to substantially alter the collisional properties of ultracold Sr. Changes in the elastic collision cross section agree well with theory for an OFR, but the inelastic collision rate constant is larger than expected. Our measurements show that a laser intensity of 20 W/cm^2 at ± 10 GHz detuning produces $\pm 10\, a_0$ of tunability in a and an estimated 1 s lifetime at a density of 10^{14} cm^{-3}. Larger laser intensity and detuning are required to use an OFR for significant increase in evaporative cooling efficiency, but the performance already demonstrated is sufficient to make an OFR near an intercombination line a powerful tool for modifying the non-linear interactions between ultracold atoms.

† These authors contributed equally to the work.

[1] I. Bloch, J. Dalibard, and W. Zwerger, Rev. of Mod. Phys. **80**, 885 (2008).
[2] M. Greiner, C. A. Regal, and D. S. Jin, Nature **426**, 537 (2003).
[3] S. Jochim, M. Bartenstein, A. Altmeyer, G. Hendl, S. Riedl, C. Chin, J. H. Denschlag, and R. Grimm, Science **302**, 2101 (2003).
[4] C. Chin, R. Grimm, P. Julienne, and E. Tiesinga, arXiv:0812.1496 (2008).
[5] P. O. Fedichev, Y. Kagan, G. V. Shlyapnikov, and J. T. M. Walraven, Phys. Rev. Lett. **77**, 2913 (1996).
[6] F. K. Fatemi, K. M. Jones, and P. D. Lett, Phys. Rev. Lett. **85**, 4462 (2000).
[7] M. Theis, G. Thalhammer, K. Winkler, M. Hellwig, G. Ruff, R. Grimm, and J. H. Denschlag, Phys. Rev. Lett. **93**, 123001 (2004).
[8] G. Thalhammer, M. Theis, K. Winkler, R. Grimm, and J. H. Denschlag, Phys. Rev. A **71**, 033403 (2005).
[9] K. Enomoto, K. Kasa, M. Kitagawa, and Y. Takahashi, Phys. Rev. Lett. **101**, 203201 (2008).
[10] H. Saito and M. Ueda, Phys. Rev. Lett. **90**, 040403 (2003).
[11] M. I. Rodas-Verde, H. Michinel, and V. M. Pérez-García, Phys. Rev. Lett. **95**, 153903 (2005).
[12] M. P. A. Fisher, P. B. Weichman, G. Grinstein, and D. S. Fisher, Phys. Rev. B **40**, 546 (1989).
[13] D. M. Bauer, M. Lettner, C. Vo, G. Rempe, and S. Durr, Nature **5**, 339 (2009).
[14] R. Ciurylo, E. Tiesinga, and P. S. Julienne, Phys. Rev. A **71**, 030701(R) (2005).
[15] R. Ciurylo, E. Tiesinga, and P. S. Julienne, Phys. Rev. A **74**, 022710 (2006).
[16] A. Stein, H. Knöckel, and E. Tiemann, Phys. Rev. A **78**, 042508 (2008).
[17] S. B. Nagel, P. G. Mickelson, A. D. Saenz, Y. N. Martinez, Y. C. Chen, T. C. Killian, P. Pellegrini, and R. Côté, Phys. Rev. Lett. **94**, 083004 (2005).
[18] P. G. Mickelson, Y. N. Martinez, A. D. Saenz, S. B. Nagel, Y. C. Chen, T. C. Killian, P. Pellegrini, and R. Cote, Phys. Rev. Lett. **95**, 223002 (2005).
[19] T. Zelevinsky, M. M. Boyd, A. D. Ludlow, T. Ido, J. Ye, R. Ciurylo, P. Naidon, and P. S. Julienne, Phys. Rev. Lett. **96**, 203201 (2006).
[20] Y. N. Martinez de Escobar, P. G. Mickelson, P. Pellegrini, S. B. Nagel, A. Traverso, M. Yan, R. Côté, and T. C. Killian, Phys. Rev. A **78**, 062708 (2008).
[21] S. Friebel, C. D'Andrea, J. Walz, M. Weitz, and T. W. Hänsch, Phys. Rev. A **57**, R20 (1998).
[22] D. Comparat, A. Fioretti, G. Stern, E. Dimova, B. Laburthe Tolra, and P. Pillet, Phys. Rev. A **73**, 043410 (2006).
[23] O. J. Luiten, M. W. Reynolds, and J. T. M. Walraven, Phys. Rev. A **53**, 381 (1996).
[24] R. deCarvalho and J. Doyle, Phys. Rev. A **70**, 053409 (2004).
[25] W. Ketterle and N. J. van Druten, Adv. Atom. Mol. Opt. Phys. **37**, 181 (1996).
[26] M. Yan, R. Chakraborty, P. G. Mickelson, Y. N. M. de Escobar, and T. C. Killian, arXiv:0905.2223 (2009).
[27] D. A. McQuarrie, Statistical Mechanics (University Science Books, Sausalito, 2000).

Acknowledgements

We thank P. Julienne for helpful discussions. This research was supported by the Welch Foundation (C-1579), National Science Foundation (PHY-0555639), and the Keck Foundation.